

^{11}B and ^{27}Al NMR spin-lattice relaxation and Knight shift study of $\text{Mg}_{1-x}\text{Al}_x\text{B}_2$. Evidence for anisotropic Fermi surface.

G. Papavassiliou¹, M. Pissas¹, M. Karayanni¹, M. Fardis¹, S. Koutandos¹, and K. Prassides^{1,2}

¹*Institute of Materials Science, NCSR, Demokritos, 153 10 Aghia Paraskevi, Athens, Greece*

²*School of Chemistry, Physics and Environmental Science, University of Sussex, Brighton BN1 9QJ, UK*

(Dated: October 31, 2018)

We report a detailed study of ^{11}B and ^{27}Al NMR spin-lattice relaxation rates ($1/T_1$), as well as of ^{27}Al Knight shift (K) of $\text{Mg}_{1-x}\text{Al}_x\text{B}_2$, $0 \leq x \leq 1$. The obtained $(1/T_1T)$ and K vs. x plots are in excellent agreement with ab initio calculations. This asserts experimentally the prediction that the Fermi surface is highly anisotropic, consisting mainly of hole-type 2-D cylindrical sheets from bonding $2p_{x,y}$ boron orbitals. It is also shown that the density of states at the Fermi level decreases sharply on Al doping and the 2-D sheets collapse at $x \approx 0.55$, where the superconductive phase disappears.

PACS numbers: 74.25.-q., 74.72.-b, 76.60.-k, 76.60.Es

The discovery of superconductivity in MgB_2 attained recently a lot of interest [1], as this binary alloy reveals a remarkably high $T_c \approx 40\text{K}$. MgB_2 is isostructural and iso-electronic with intercalated graphite (ICG), with carbon replaced by boron, and therefore exhibits similar bonding and electronic properties as ICG. Thus the high T_c value of MgB_2 in comparison to ICG ($\sim 5\text{K}$) was very surprising.

Band structure calculations [2, 3, 4, 5, 6] have shown that Mg is substantially ionized in this compound, however the electrons donated to the system are not localized on the B anion, but rather are distributed over the whole crystal. The six B p bands contribute mainly at the Fermi level. The unique feature of MgB_2 is the incomplete filling of the two σ bands corresponding to prominently covalent sp^2 -hybridized bonding within the graphite-like boron layer. Two isotropic π bands are derived from B p_z states and four two dimensional σ -bands from B $p_{x,y}$. Both p_z bands cross the Fermi level, while only two bonding $p_{x,y}$ bands and only near the Γ point (0,0,0) do so, forming cylindrical Fermi surfaces around Γ -A line. Due to their 2D character, these bands contribute more than 30% to the total density of states (DOS)[2, 4, 7, 8]. Such strong anisotropy in the Fermi surface (and possibly in the electron phonon coupling) conciles with the recently reported anisotropy in H_{c2} [9, 10, 11, 12, 13, 14], and the existence of two superconducting gaps [15, 16, 17, 18, 19, 20, 21].

In view of these important findings, great interest has been raised on measurements of electron or hole doped MgB_2 , aiming to clarify how the electron DOS and the Fermi surface depend on doping. A very suitable substitution for such a study is Al, which donates three electrons (instead of two for Mg), and thus doping by one electron per atom. In addition, the end members MgB_2 and AlB_2 as well as the intermediate mixed crystals $\text{Mg}_{1-x}\text{Al}_x\text{B}_2$ crystallize in the $P6/mmm$ space group, whereas by Al doping the lattice constants decrease almost linearly [22]. The similarity of the calculated elec-

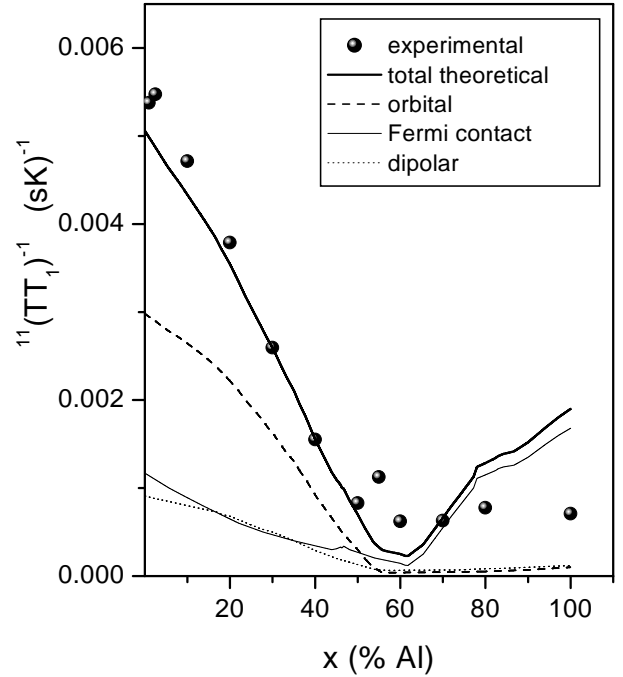


FIG. 1: Boron $^{11}(1/T_1T)$ for $\text{Mg}_{1-x}\text{Al}_x\text{B}_2$ as a function of Al-doping. Lines show the ab initio calculated plots from Refs. 4, 8

tronic density of states between MgB_2 and AlB_2 indicates that Al doping results in simple filling of the available electronic states. Suzuki *et al.* [23] predicted that in $\text{Mg}_{1-x}\text{Al}_x\text{B}_2$ the concentration of σ holes varies with x as $n_h = (0.8 - 1.4x) \times 10^{22} \text{ cm}^{-3}$, leading to $n_h = 0$ for $x \approx 0.6$. A similar conclusion was deduced in Refs. 3, 4, 24. Under these aspects, the detrimental effect of Al doping on T_c can be explained by the fact that doping increases the Fermi energy (E_F), while decreasing the DOS $N(E_F)$.

An excellent probe to study the influence of the Al sub-

stitution on the electronic structure of electron doped MgB_2 is nuclear magnetic resonance (NMR). Knight shift, K , and nuclear spin-lattice relaxation (NSLR) rate $1/T_1$ measurements, give us the possibility to determine experimentally $N(E_F)$ through the static and fluctuating parts of the hyperfine field, induced at the position of the resonating nuclei from electrons at the Fermi surface. This allows to estimate the contribution of different atoms to $N(E_F)$ as well as and the anisotropy of electronic states at the Fermi level.

The Hamiltonian describing the magnetic interaction of the nucleus with the atomic electrons can be written as [25]: $\mathcal{H} = 2(8\pi/3)\mu_B\gamma_n\hbar\mathbf{I}\cdot\mathbf{S}(\mathbf{r})\delta(\mathbf{r}) - 2\mu_B\gamma_n\hbar\mathbf{I}\cdot[\mathbf{S}/r^3 - 3\mathbf{r}(\mathbf{S}\cdot\mathbf{r})/r^5] - \gamma_n\hbar(e/mc)[\mathbf{I}\cdot(\mathbf{r}\times\mathbf{p})/r^3]$, where μ_B is the Bohr magneton, γ_n the gyromagnetic ratio, \mathbf{I} and \mathbf{S} the nuclear and electron spins respectively, and \mathbf{r} is the radius vector of the electron with the nucleus at the origin. In the formula above, the first term describes the Fermi contact interaction, the second term the spin dipolar interaction between nuclear and electron spins, and the third term the coupling with the electronic orbital moment. In the simplest case, where only contribution from the Fermi contact term is considered, the first term can be rewritten as $\mathcal{H}_{KS} \propto -V(8\pi/3)\gamma_n\hbar\chi_p\langle|\Psi(0)|^2\rangle_{F_S}\mathbf{I}\cdot\mathbf{H}_0$, where $\chi_p = M/H = \mu_B^2N_s(E_F)/V$, and the symbol $\langle\rangle_{F_S}$ means the average over all s orbitals at the Fermi surface. Due to this term the nuclear spin \mathbf{I} 'sees' an internal field $V\chi_p\mathbf{H}_0/2\mu_B$, which is superimposed on the applied external magnetic field, and causes a paramagnetic shift of the nuclear resonance, i.e. the Knight shift. In a similar way, the relaxation rate from the Fermi contact term is expressed by the relation [25]: $(1/T_1) = (64\pi^3/9)\gamma_e^2\gamma_n^2\hbar^3\langle|\Psi_{\mathbf{k}}(0)|^2|\Psi_{\mathbf{k}'}(0)|^2\rangle_F N_s(E_F)^2 k_B T$. A similar dependence on $N_{2p}(E_F)^2$ holds if the nuclear Hamiltonian is dominated by the nuclear-electron orbital interaction [26]. Hence, the dependence of both K and $1/T_1$ on certain partial $N_i(E_F)$ is clear.

Until now, ^{11}B , ^{27}Al and ^{25}Mg NSLR and Knight shift measurements have been reported for pure MgB_2 and AlB_2 [27, 28, 29, 30, 31], which are in agreement with the theoretical predictions. These results, in conjunction with ab initio calculations [4, 7, 8] have shown that in MgB_2 the ^{11}B NSLR is dominated by orbital relaxation, whereas in AlB_2 the ^{11}B NSLR is overruled by the Fermi-contact interaction. On the other hand, ^{27}Al and ^{25}Mg NSLRs, as well as the Knight shift on all three ^{11}B , ^{27}Al , and ^{25}Mg sites was shown to be controlled by the Fermi-contact polarization [7, 29]. Besides, ^{11}B -NMR NSLR relaxation rate measurements on mixed $\text{Mg}_{1-x}\text{Al}_x\text{B}_2$, $x \leq 0.2$, have shown a rapid decrease of $1/(T_1T)$ with doping that was attributed to reduction of the total $N(E_F)$ [32]. Nevertheless, a detailed NMR study of the variation of each partial $N_i(E_F)$ with Al doping, and comparison with theory is lacking so far.

The purpose of this work is to report a systematic study of ^{11}B and ^{27}Al NSLR rates $1/T_1$, as well as of ^{27}Al

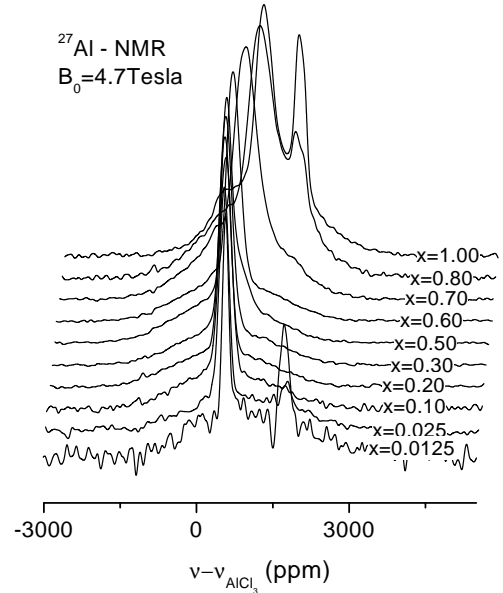


FIG. 2: ^{27}Al NMR line shapes of the central transition at room temperature for $\text{Mg}_{1-x}\text{Al}_x\text{B}_2$. For $x = 0.0125$ and 0.025 100,000 accumulations were acquired, due to the weakness of the signals. In the low doping regime, the spurious signal at +1700 ppm is coming from the probe. The peak at the same frequency for $x = 0.80, 1.0$ is produced by free Al that unavoidably remained during sample preparation. For clarity, all spectra are normalized to one.

Knight shifts, as a function of Al doping for $\text{Mg}_{1-x}\text{Al}_x\text{B}_2$, $0 \leq x \leq 1$. ^{11}B Knight shift measurements were not considered, because the isotropic ^{11}B Knight shift is small (+40 ppm for MgB_2 and -10 ppm for AlB_2 [29]), and of the same order of magnitude with the dipolar and the second order quadrupolar split in the NMR fields 2.35, and 4.7 Tesla that have been used in this work. Our measurements show an excellent agreement between the experimental boron $^{11}(1/T_1T)$ plot with that obtained from local density-functional methods [4, 8], and the dominance of the orbital relaxation up to $x \approx 0.55$, where $T_c(x)$ vanishes. This is a convincing evidence that up to this doping the hole-type 2-D cylindrical sheets (from bonding $2p_{x,y}$ boron orbitals) of the Fermi surface play an essential role in the ^{11}B NSLR. The slight decrease of both ^{27}K and $^{27}(1/T_1T)$ for $x \leq 0.55$, and their abrupt increase above this doping value are in support of this conclusion.

Polycrystalline samples of nominal composition $\text{Mg}_{1-x}\text{Al}_x\text{B}_2$ for $0 \leq x \leq 1$ were prepared by reaction of Al and Mg powders with amorphous B at temperatures between 700°C and 910°C as described elsewhere [14]. We notify that: According to the available literature [22, 33, 34, 35] and our data, the temperature where the reaction (preparation temperature) takes place, defines the shape of the (00l) diffraction peaks in the region

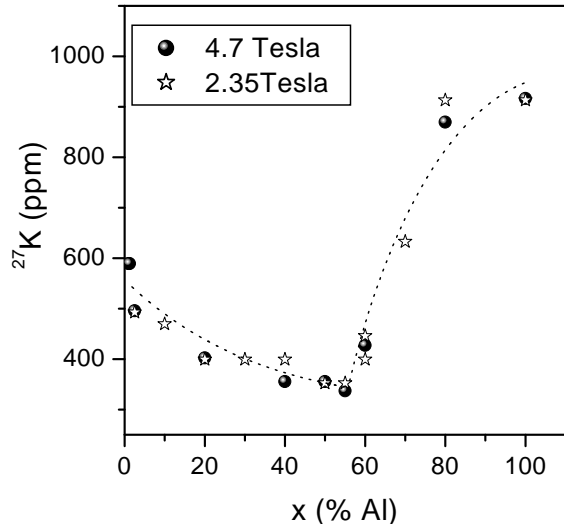


FIG. 3: The ^{27}K Knight shift of NMR spectra for $\text{Mg}_{1-x}\text{Al}_x\text{B}_2$ in fields 2.35 and 4.7 Tesla.

$0.05 \leq x \leq 0.5$. The existence of significant broadening or/and splitting in these peaks manifest the existence of some kind of phase separation in this doping range. (ii) Carefully prepared samples in the region around $x = 0.5$ display a broad superlattice peak (001/2) which means that ordering of Mg and Al occurs [36].

^{27}Al NMR line shape measurements of the central transition ($-1/2 \rightarrow 1/2$) were performed on two spectrometers operating in external magnetic fields $H_0 = 2.35$ and 4.7 Tesla. Spectra were obtained from the Fourier transform of half of the echo, following a typical $\pi/2 - \tau - \pi/2$ solid spin-echo pulse sequence. The ^{11}B T_1 of the central line was determined by applying a saturation recovery technique, and fitting with the two exponential relaxation function that is appropriate for $I = 3/2$ nuclei [37]. Correspondingly, ^{27}Al T_1 was determined by applying the three-exponential recovery law that is appropriate for $I = 5/2$ nuclei [30, 37].

Figure 1 shows the boron $^{11}(1/TT_1)$ as a function of x , in the normal state. In all cases a single component of T_1 was found to fit satisfactorily the magnetization recovery curves. Besides, a $1/T_1T = \text{constant}$ relation was fitting the experimental data from room temperature down to 80K. Our measurements reveal that by increasing doping, $^{11}(1/TT_1)$ decreases rapidly up to $x = 0.55$, and subsequently exhibits a slight increase for $x \geq 0.55$. For reasons of comparison, we have plotted the calculated $^{11}(1/TT_1)$ values from Ref. 8, for all three orbital, dipole-dipole, and Fermi contact term contributions. Clearly, the orbital term dominates in the ^{11}B relaxation rates for $x \leq 0.55$. In case of pure MgB_2 the ^{11}B orbital hyperfine interaction of $2p$ -holes with the nuclear magnetic moments is about 3 times larger than the dipole-dipole,

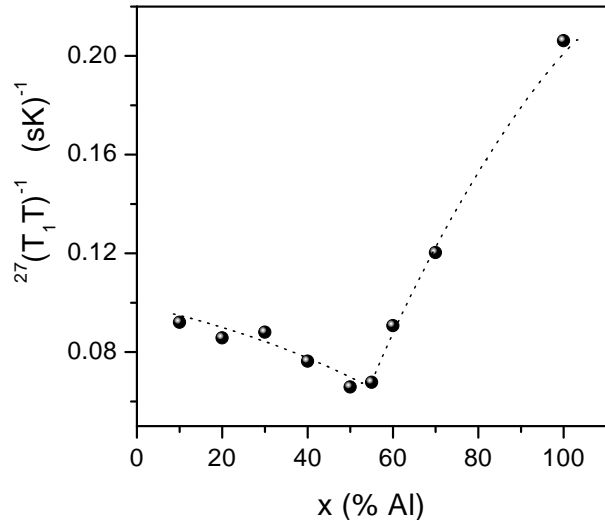


FIG. 4: $^{27}(1/T_1T)^{-1}$ for $\text{Mg}_{1-x}\text{Al}_x\text{B}_2$ as a function of Al-doping x .

and the Fermi contact interaction. This is due to the fact that the boron p_σ and p_π bands are all at the Fermi level ($N_{px}=N_{py} \approx 0.035$, $N_{pz} \approx 0.045$ states/eV/spin/B), whereas only a few s boron electrons are close to the Fermi level ($N_s \approx 0.002$ states/eV/B)[7, 29]. This gives a ratio between the Fermi-contact and the orbital/dipole-dipole coupling constants, $F \simeq 0.35$ [7], and $^{11}T_1^{-1}$ is mainly proportional to $N_{2p}(E_F)^2$. It may thus be inferred that the rapid decrease of the ^{11}B relaxation rate is due to decrease of the DOS in the $2-D$ hole-type sheets, while a minimum $1/T_1$ value is obtained at $0.55 \leq x \leq 0.60$, where the $2-D$ sheets appear to collapse. We also notice the discrepancy between the theoretical and experimental values for $x > 0.6$. Most probably, calculations tend to overestimate the Fermi contact interaction at the position of the B nucleus in this doping range [29].

Figure 2 demonstrates ^{27}Al NMR line shapes of $\text{Mg}_{1-x}\text{Al}_x\text{B}_2$ at room temperature in field 4.7 Tesla. A completely similar picture was obtained in field 2.35 Tesla. The spectra for $x = 0.0125$, and 0.025 , were extremely weak, and therefore were acquired with 100,000 signal accumulations (for comparison, signals for $x \geq 0.1$ were acquired with 512 accumulations). In all samples the spectra consist of a central transition line, ≈ 20 kHz wide, which shifts with doping, and a broad powder pattern from the satellite transitions. The low doping spectra exhibit a spurious weak peak at +1700 ppm that was produced by the probe. The strong peak at the same frequency for $x = 0.80, 1.0$ is produced by free Al that unavoidably remains during sample preparation at high doping concentrations.

In Figure 3 we show the shift of the central line peak as a function of x , in fields 2.35 and 4.7 Tesla. The sig-

nal of a standard aqueous solution of AlCl_3 was used as reference. The coincidence of the curves in both fields is a clear evidence that the obtained spectral shift corresponds solely to the ^{27}K shift. In typical metallic shifts of $I = 5/2$ nuclei like ^{27}Al , in addition to the Knight shift, the center-of-gravity position of the NMR signal should include the second-order quadrupole shift given by $\Delta\nu = (25\nu_Q^2)/(18\nu_L)$ [38]. However, recent experiments on AlB_2 have shown that the quadrupolar coupling constant is $\nu_Q \simeq 80$ kHz [29], thus giving a negligibly small second order quadrupolar shift, $\Delta\nu \approx 14$ ppm. According to Figure 3, by increasing x the ^{27}K decreases rapidly, whereas for $x \geq 0.55$, i.e. at the doping value where the superconductive phase disappears [24], it increases sharply becoming $\approx +900$ ppm for pure AlB_2 . As previously shown, by Al doping of MgB_2 the σ hole bands are filled [3, 4, 24], and their contribution to $N(E_F)$ becomes zero at $x \approx 0.55$ [24]. Evidently, the gradual decrease of ^{27}K for $x \leq 0.55$ reflects, (i) the initial slight decrease of $N_s(E_F)$ in this doping range [2], and (ii) the reduction of the Stoner enhancement by filling the σ hole bands, due to decrease of the total $N(E_F)$. We notice that the Stoner enhancement renormalizes both K and $1/T_1$ by a factor $S = 1/(1 - IN(E_F))^\alpha$, with $\alpha = 1$ for K , and $1 \leq \alpha \leq 2$ for $1/T_1$ [7, 8]. On the other hand, the sharp increase of the Knight shift for $x \geq 0.55$, may be attributed to the rapid increase of N_s by further doping, after completely filling the $2p_{x,y}$ hole bands ($N_s(\text{Mg})$ in MgB_2 is ≈ 0.0092 states/eV/spin, whereas $N_s(\text{Al})$ in AlB_2 is ≈ 0.0362 states/eV/spin [7]). A similar behaviour is observed in Figure 4, which exhibits the $^{27}(1/\text{TT}_1)$ vs. x plot. This is expected as the ^{27}Al relaxation rate is dominated by the Fermi contact interaction, and therefore is proportional to $N_s^2(\text{Al})$ [29].

In conclusion, ^{11}B and ^{27}Al NMR NSLR rate and Knight shift measurements have been employed in order to investigate the structure and the variation of the Fermi surface in MgB_2 upon Al (i.e. electron) doping. Our results are completely consistent with calculations predicting a strongly anisotropic Fermi surface that is comprised from hole-type σ -bonding $2 - D$ cylindrical sheets, and a hole-type and electron-type, $3 - D$ π -bonding tubular network. The collapse of the $2 - D$ sheets at $x \simeq 0.55$, as predicted by theory, is experimentally verified by the fast decrease of the ^{11}B NSLR rate for $x \leq 0.55$ and the sharp increase of both the ^{27}K , and $^{27}\text{NSLR}$ rates for $x \geq 0.55$. The latter indicates a strong reshaping of the Fermi surface towards the electronic structure of AlB_2 ,

due to interplane electron contribution. Our results conciliate with both experimental and theoretical evidence that indicate anisotropic pairing and multi-gap superconductivity in MgB_2 .

-
- [1] J. Nagamatsu *et al.*, Nature(London) **410**, 63 (2001).
 - [2] J. Cortus *et al.*, Phys. Rev. Lett. **86**, 4656 (2001).
 - [3] J. M. An and W. E. Pickett, Phys. Rev. Lett. **86**, 4366 (2001).
 - [4] K. D. Belashchenko *et al.*, Phys. Rev. B **64**, 092503 (2001); V. P. Antropov *et al.*, cond-mat/0107123.
 - [5] Y. Kong *et al.*, Phys. Rev. B **64** 020501(R) (2001).
 - [6] P. P. Singh, Phys. Rev. Lett. **87**, 087004 (2001).
 - [7] E. Pavarini *et al.*, Phys. Rev. B. **64**, 140504 (2002).
 - [8] K. D. Belashchenko *et al.*, Phys. Rev. B. **64**, 132506 (2001).
 - [9] O. F. de Lima *et al.*, Phys. Rev. Lett. **86**, 5974 (2001).
 - [10] S. Patnaik *et al.*, Supercond. Sci. Technol. **14**, 315 (2001).
 - [11] F. Simon *et al.*, Phys. Rev. Lett. **87**, 047002 (2001).
 - [12] S. L. Bud'ko *et al.*, cond-mat/0106577 (2001).
 - [13] G. Papavassiliou *et al.*, Phys. Rev. B **65**, 012510 (2002).
 - [14] M. Pissas *et al.*, Phys. Rev. B, in press.
 - [15] F. Bouquet *et al.*, Phys. Rev. Lett. **87**, 047001 (2001).
 - [16] Amy Y. Liu *et al.*, Phys. Rev. Lett. **87**, 087005 (2001).
 - [17] P. Szabo *et al.*, Phys. Rev. Lett. **87**, 137005 (2001).
 - [18] X. K. Chen *et al.*, Phys. Rev. Lett. **87**, 157002 (2001).
 - [19] S. Tsuda *et al.*, Phys. Rev. Lett. **87**, 177006 (2001).
 - [20] F. Giubileo *et al.*, Phys. Rev. Lett. **87**, 177008 (2001).
 - [21] H. D. Yang *et al.*, Phys. Rev. Lett. **87**, 167003 (2001).
 - [22] J. S. Slusky *et al.*, Nature (London) **410**, 343 (2001).
 - [23] S. Suzuki *et al.*, J. Phys. Soc. Jpn. **70**, 1206 (2001).
 - [24] O. de la Pena *et al.*, cond-matt/0203003 (2002).
 - [25] *Principles of Nuclear Magnetism*, A. Abragam, Oxford university press (1999).
 - [26] Y. Obata, J. Phys. Soc. Jpn. **18**, 1020 (1963); T. Asada and K. Terakura, J. Phys. F **12**, 1387 (1982).
 - [27] H. Kotegawa *et al.*, Phys. Rev. Lett. **87**, 127001 (2001).
 - [28] J. K. Jung *et al.*, Phys. Rev. B. **64**, 012514 (2001).
 - [29] S. H. Baek *et al.*, cond-matt/0201450 (2002).
 - [30] M. Mali *et al.*, Phys. Rev. B. **65**, 100518 (2002).
 - [31] A. P. Gerashenko *et al.*, Phys. Rev. B. **65**, 132506 (2002).
 - [32] H. Kotegawa *et al.*, cond-matt/0201578 (2002).
 - [33] J. Y. Xiang *et al.*, cond-matt/0104366 (2002).
 - [34] JJ. Q. Li *et al.*, Phys. Rev. B. **65**, 132505 (2002).
 - [35] H. W. Zanbergen *et al.*, Physica C **360**, 221 (2002).
 - [36] S. Margadonna *et al.*, cond-matt/0204015 (2002).
 - [37] E. R. Andrew and D. P. Tunstall, Proc. Phys. Soc. London **78**, 1 (1961).
 - [38] M. H. Cohen and F. Reif, in Solid State Physics: Advances in Research and Applications, edited by F. Seitz and D. Turnbull (Academic Press, New York, 1957), Vol. 5.